Geometric Factors of Bipole-Dipole Arrays

GEOLOGICAL SURVEY BULLETIN 1313-B

Geometric Factors of Bipole-Dipole Arrays

By ADEL A. R. ZOHDY

NEW TECHNIQUES IN DIRECT-CURRENT RESISTIVITY EXPLORATION

GEOLOGICAL SURVEY BULLETIN 1313-B

Nomograms, curves, and tables simplify evaluation of geometric factors of azimuthal, perpendicular, and parallel bipole-dipole electrode arrangements for measuring electrical resistivities of the earth

UNITED STATES GOVERNMENT PRINTING OFFICE, WASHINGTON : 1970

UNITED STATES DEPARTMENT OF THE INTERIOR

WALTER J. HICKEL, *Secretary*

GEOLOGICAL SURVEY

William T. Pecora, *Director*

Library of Congress catalog-card No. 73-607298

For sale by the Superintendent of Documents, U.S. Government Printing Office
Washington, D.C. 20402 - Price 25 cents (paper cover)

CONTENTS

ILLUSTRATIONS

TABLES

NEW TECHNIQUES IN DIRECT-CURRENT RESISTIVITY EXPLORATION

GEOMETRIC FACTORS OF BIPOLE-DIPOLE ARRAYS

By ADEL A. R. ZOHDY

ABSTRACT

Formulas are derived for computing the geometric factors of the azimuthal, equatorial, parallel, polar, perpendicular, and L-shaped bipole-dipole electrode arrays. The derivations are based on the assumption that a component of the electric field along the azimuthal, the parallel, or the perpendicular direction is approximately measured. For each array, the geometric factor is expressed as the product of two factors, K^* and A. The factor K^* is simple to compute, being expressed as (R^2/MN) for all the considered arrays where R is the bipole-dipole spacing and MN is the distance between the measuring electrodes. The expression for the factor A is complicated, and its evaluation is generally cumbersome. Nomograms, curves, and tables are given to facilitate the evaluation of the various A factors with sufficient accuracy for most practical purposes.

INTRODUCTION

Several electrode arrangements are known to geophysicists engaged in electrical prospecting. The preference of one arrangement over another is partially governed by the simplicity of the expression of the geometric factor, K. For example, one of the simplest geometric factor expressions is that of the well-known Wenner arrangement, $K_W=2\pi a$, where a is the distance between the equally spaced electrodes A, M, N, and B (A and B are current electrodes; M and N are potential electrodes). In the practical $AMNB$-Schlumberger array, the geometric factor, K_S, is more complex and is given by $K_S=\pi[(AB/2)^2-(MN/2)^2]/MN$, where $AB \geq 5MN$. In practice, one or more tables of precalculated values for K_S are used to facilitate the computation of the apparent resistivity, $\bar{\rho}_S$, from the well-known general formula

$$\bar{\rho}_S=K_S\frac{\Delta V}{I},$$

where ΔV is the measured voltage (between M and N) and I is the electric current. For a given distance between current electrodes, AB, and a given current intensity, I, one measures a smaller potential difference, ΔV, when using the Schlumberger array than when using the Wenner array. This is mathematically expressed in an inverse relationship for the corresponding geometric factors. Thus more current is required when using the Schlumberger than when using the Wenner array to produce the same ΔV at the same AB. However, the sensitivity of the Schlumberger array for detecting a given layer, at a given depth and at a given AB, is greater than that of the Wenner array (Deppermann, 1954: Zohdy, 1964).

In recent years, the possibility of making electrical soundings using dipole-dipole arrays (Al'pin, 1950) has received considerable attention (Alekseev and others, 1957; Anderson and Keller, 1966; Cantwell and others, 1965; Cantwell and Orange, 1965; Berdichevskii, 1957; Berdichevskii and Zagarmistr, 1958; Jackson, 1966). The expressions for the geometric factors of the various dipole-dipole arrays are not particularly complex, but the magnitudes of these geometric factors are large and increase very rapidly as the spacing between the centers of the two dipoles is increased. The large values of these dipole-dipole geometric factors reflect the requirement for tremendous electric power and a high-sensitivity potential-measuring instrument. Using bipole-dipole arrays instead of dipole dipole arrays overcomes these prohibitive requirements. In a bipole-dipole array, the distance, R, between the centers, Q and O, of the bipole and the dipole is not exceedingly larger than $AB/2$, that is, $R \leq 10(AB/2)$; and the length of the current bipole, AB, is large in comparison to that of the measuring dipole, MN (fig. 1). Geometric factors of bipole-dipole arrays are generally smaller in magnitude but more complex in form than those of corresponding ideal dipole-dipole arrays.

In general, the value of the geometric factor for any quadrupole array can be computed from the expression (Heiland, 1946)

$$\rho = \frac{2\pi}{\left(\frac{1}{r_1} - \frac{1}{r_2} - \frac{1}{r_3} + \frac{1}{r_4}\right)} \frac{\Delta V}{I},$$

where r_1, r_2, r_3, and r_4 are the distances AM, AN, BM, and BN between the current electrodes, A and B, and the potential electrodes, M and N. In electrical sounding using bipole-dipole or dipole-dipole arrays, AM nearly equals AN and BM nearly equals BN; therefore the calculation of ρ from the above equation requires the measurement of AM, AN, BM, and BN with great accuracy. Furthermore, by expressing the distances AM, AN, BM, and BN in terms of quantities (AB, MN, R, and θ) that are readily measured in the field, the expres-

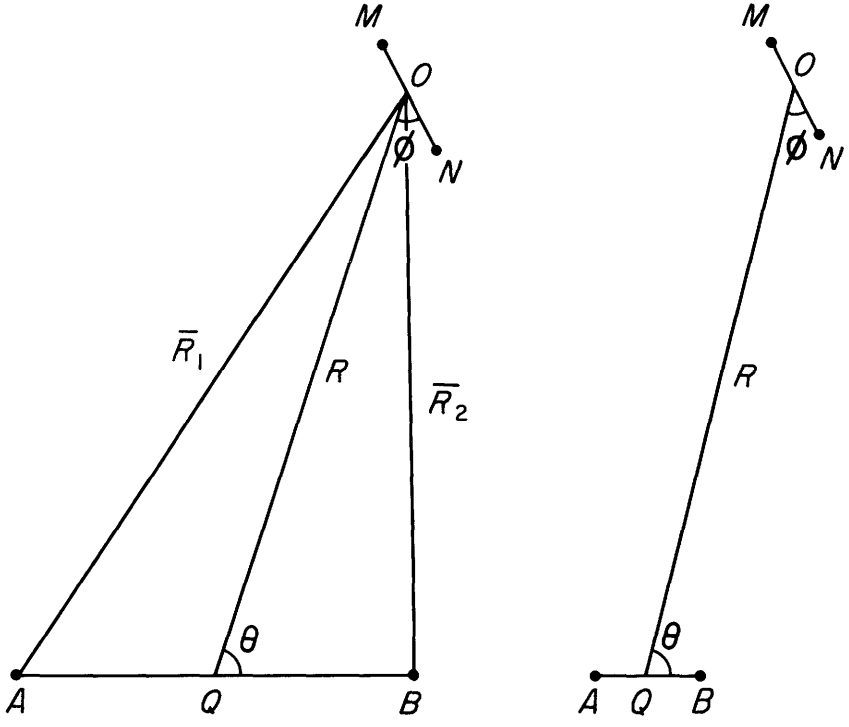

FIGURE 1.—Bipole-dipole (*left*) and dipole-dipole (*right*) arrays. *A* and *B*, current electrodes; *Q*, center of current bipole (*left*) or dipole (*right*); *M* and *N*, measuring electrodes; *O*, center of measuring dipole; *R*, distance between centers of bipole and dipole; $\bar{R}$, distance between center of dipole and current electrode.

sion of the geometric factor using the above equation becomes very complicated for nonlinear bipole-dipole arrays. To simplify the computation of the geometric factor of bipole-dipole arrays, the apparent resistivity is expressed in terms of the electric field, E, instead of the potential difference, ΔV, and then the approximation $E=\Delta V/MN$ is used.

The use of bipole-dipole arrangements for making electrical soundings poses problems in the presentation and interpretation of the sounding data. Difficulties arise because of the introduction of additional variables not present in dipole-dipole, Schlumberger, or Wenner arrays. These variables are the azimuth angle, θ and the finite length of the bipole, AB. The problems arising from the introduction of these variables are not mathematically formidable, at least for horizontally stratified media, where the sounding data may be processed in part by using "effective spacing factors," "effective resistivity factors," or other transformation procedures. The development of these types of

analyses, however, is beyond the scope of this paper. With the exception of the equatorial array, the following discussion will be concerned only with the first fundamental problem, namely simplifying the computation of the geometric factors so that the magnitude of the resistivity can be evaluated easily.

The author thanks Donald Plouff and Paul G. Hoffman, of the U.S. Geological Survey, for writing the necessary programs for the CDC–3600 computer.

GEOMETRIC FACTOR OF THE AZIMUTHAL ARRANGEMENT

In the azimuthal arrangement, the perpendicularity of MN to R is maintained at all times, or $\phi = \pi/2$ (fig. 1). An electrical sounding can be made by varying the distances R, AB, and (or) the angle θ.[1] The general formula for computing the apparent resistivity, using the azimuthal arrangement, is given by

$$\overline{\rho}_\theta = K_\theta \frac{\Delta V_{MN}^{A,B}}{I}, \tag{1}$$

where

$\overline{\rho}_\theta$ = resistivity measured by the azimuthal arrangement,
K_θ = geometric factor of the azimuthal arrangement,
$\Delta V_{MN}^{A,B}$ = potential difference between the measuring electrodes M and N (placed around the point O) due to the current electrodes A and B, and
I = intensity of the electric current.

If MN is sufficiently small in comparison to AO and BO ($AO \geq 10\ MN$, $BO \geq 10\ MN$), then the electric field component at the point O, along the direction MN, is approximately measured. In other words,

$$\lim_{MN \to 0} \frac{\Delta V}{MN} = \frac{dV}{d(MN)} = E_{MN}|_o = E_\theta|_o,$$

or

$$\Delta V_{MN}^{A,B} \simeq MN\ E_\theta|_o, \tag{2}$$

where

$E_{MN}|_o = E_\theta|_o$ = azimuthal component of the electric field at the point O, along the azimuthal direction, θ, of MN.

Let R and $\overline{R}$ be the distances from the center Q of AB and from a point electrode, respectively, to a given point on the earth's surface where the electric field is measured. The magnitude of the azimuthal component of the electric field, E_θ, at the point O (fig. 2) is given by

$$E_\theta = E_{MN}^{A,B}\Big|_o = E_{\overline{R}_1}^{A}\Big|_o \cos\alpha + E_{\overline{R}_2}^{B}\Big|_o \cos\beta, \tag{3}$$

[1] In the ideal dipole-dipole azimuthal, radial, and perpendicular (but not the parallel) arrays, the resistivity measurements are independent of the azimuth angle θ (Al'pin, 1950).

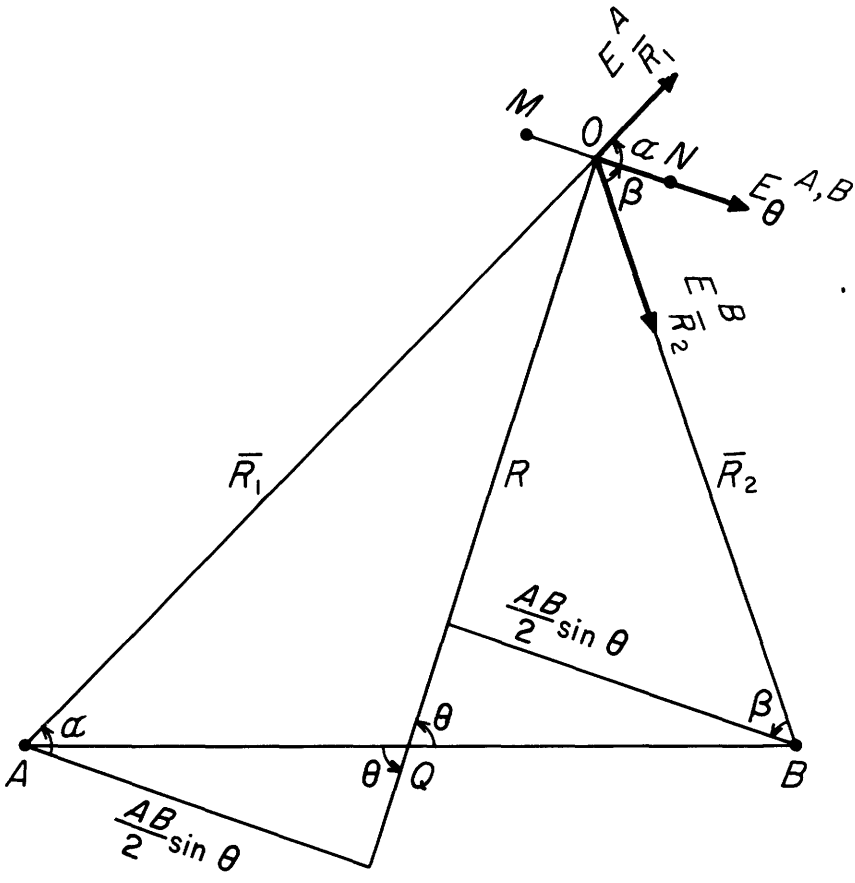

FIGURE 2.—Bipole-dipole azimuthal array. A and B, current electrodes; Q, center of current bipole; M and N, measuring electrodes; O, center of dipole; R, distance between centers of bipole and dipole; AB, distance between current electrodes; $\bar{R}$, distance between current electrode and center of dipole; E, point-source component of electric field; E_θ, azimuthal component of electric field.

where

$E_{\bar{R}_1}^A\Big|_o, E_{\bar{R}_2}^B\Big|_o$ = radial components of the electric fields, along $\bar{R}_1$ and $\bar{R}_2$, at the point O, due to the electrodes A and B, respectively,

and

α, β = the angles $(\vec{E}_{\bar{R}_1}^A, \overrightarrow{MN})$ and $(\vec{E}_{\bar{R}_2}^B, \overrightarrow{MN})$, respectively.

From figure 2, the following relationships apply:

$$\cos\alpha = \frac{(AB/2)\sin\theta}{\bar{R}_1}, \tag{4a}$$

$$\cos\beta = \frac{(AB/2)\sin\theta}{\bar{R}_2}, \tag{4b}$$

$$\bar{R}_1=\sqrt{R^2+\left(\frac{AB}{2}\right)^2+2R\left(\frac{AB}{2}\right)\cos\theta}, \tag{4c}$$

and

$$\bar{R}_2=\sqrt{R^2+\left(\frac{AB}{2}\right)^2-2R\left(\frac{AB}{2}\right)\cos\theta}. \tag{4d}$$

For a homogeneous isotropic semi-infinite medium of resistivity ρ, the radial components of the electric fields due to the point electrodes A and B, at the point 0, are given by

$$E^{A}_{\bar{R}_1}\Big|_o=\frac{\rho I}{2\pi\bar{R}_1^2} \tag{5a}$$

and

$$E^{B}_{\bar{R}_2}\Big|_o=\frac{\rho I}{2\pi\bar{R}_2^2}, \tag{5b}$$

respectively. Hence, substituting equations 4a–d and 5a,b in equation 3 and rearranging, we get

$$E_\theta\Big|_o=\frac{\rho I}{2\pi}\frac{\left(\frac{AB}{2}\right)\sin\theta}{R^3}\left(\frac{1}{\left[1+\left(\frac{AB}{2R}\right)^2+2\left(\frac{AB}{2R}\right)\cos\theta\right]^{3/2}}+\frac{1}{\left[1+\left(\frac{AB}{2R}\right)^2-2\left(\frac{AB}{2R}\right)\cos\theta\right]^{3/2}}\right). \tag{6}$$

Substituting equation 6 in equation 2, solving for ρ, and rearranging, we get

$$\rho=\frac{R^2}{MN}\frac{2\pi}{\left(\frac{AB}{2R}\right)\sin\theta}\left(\frac{1}{\left[1+\left(\frac{AB}{2R}\right)^2+2\left(\frac{AB}{2R}\right)\cos\theta\right]^{-3/2}}+\left[1+\left(\frac{AB}{2R}\right)^2-2\left(\frac{AB}{2R}\right)\cos\theta\right]^{-3/2}\right)\frac{\Delta V^{A,B}_{MN}}{I}. \tag{7}$$

In practice, for any given electrode arrangement, the apparent resistivity, $\bar{\rho}$, is calculated by using the formula derived for a homogeneous isotropic half space (whereas the actual measurements might be made over a heterogeneous generally anisotropic medium). Hence equation 7 is valid for computing the apparent resistivity by the azimuthal arrangement, and from equation 1 it follows that

$$K_\theta=\frac{R^2}{MN}\frac{2\pi}{\left(\frac{AB}{2R}\right)\sin\theta}\left(\frac{1}{\left[1+\left(\frac{AB}{2R}\right)^2+2\left(\frac{AB}{2R}\right)\cos\theta\right]^{-3/2}}+\left[1+\left(\frac{AB}{2R}\right)^2-2\left(\frac{AB}{2R}\right)\cos\theta\right]^{-3/2}\right). \tag{8}$$

The numerical evaluation of K_θ from equation 8 is cumbersome. Therefore, let

$$K_\theta = K_\theta^* A_\theta, \tag{9}$$

where

$$K_\theta^* = \frac{R^2}{MN} \tag{10}$$

and

$$A_\theta = \frac{2\pi}{\left(\frac{AB}{2R}\right)\sin\theta} \left(\frac{1}{\left[1+\left(\frac{AB}{2R}\right)^2+2\left(\frac{AB}{2R}\right)\cos\theta\right]^{-3/2} + \left[1+\left(\frac{AB}{2R}\right)^2-2\left(\frac{AB}{2R}\right)\cos\theta\right]^{-3/2}} \right). \tag{11}$$

Values of the factor A_θ, which is independent of the dipole length MN, were computed for $0.1 \leq (AB/2R) \leq 1$ and for $0° \leq \theta \leq 90°$ and contoured as shown in figure 3. An example of the evaluation of the factor A_θ, using the nomogram, follows:

Let $R=1{,}000$ meters, $AB/2=500$ meters, $MN=100$ meters, and $\theta=45°$. To determine K_θ, we first find K_θ^*:

$$K_\theta^* = \frac{R^2}{MN} = 10^4 \text{ meters.}$$

The value of A_θ as estimated from the nomogram (fig. 3), at the ordinate $AB/2R=0.5$ and the abscissa $\theta=45°$, is 6.2. Therefore $K_\theta = 6.2 \times 10^4$ meters. (If R, $AB/2$, and MN are measured in feet, then the value of K_θ must be multiplied by the conversion factor 0.3048 for the resistivity to be expressed in ohm-meters.)

In accordance with equation 11, the values of A_θ approach infinity as the orientation of the measuring dipole MN tends to coincide with an equipotential line (as, for example, at $\theta=0°$). This reflects the fact that as the potential difference between M and N becomes infinitely small, the geometric factor must become infinitely large in order that the value of ρ remain finite.

A nomogram for $0.01 \leq (AB/2R) \leq 0.3$ and $60° \leq \theta \leq 90°$ was published by Berdichevskii (1957) and by Bordovskii (1958). The expression for K_θ given by Berdichevskii is

$$K_\theta = \overset{*}{K}_\theta A_\theta,$$

where

$$\overset{*}{K}_\theta = \frac{R^3}{AB\,MN}\, 10^3 \tag{12}$$

and

$$A_\theta = \frac{4\pi}{\sin\theta} \left\{ \frac{1}{\left[1+\left(\frac{AB}{2R}\right)^2+\frac{AB}{R}\cos\theta\right]^{-3/2} + \left[1+\left(\frac{AB}{2R}\right)^2-\frac{AB}{R}\cos\theta\right]^{-3/2}} \right\}. \tag{13}$$

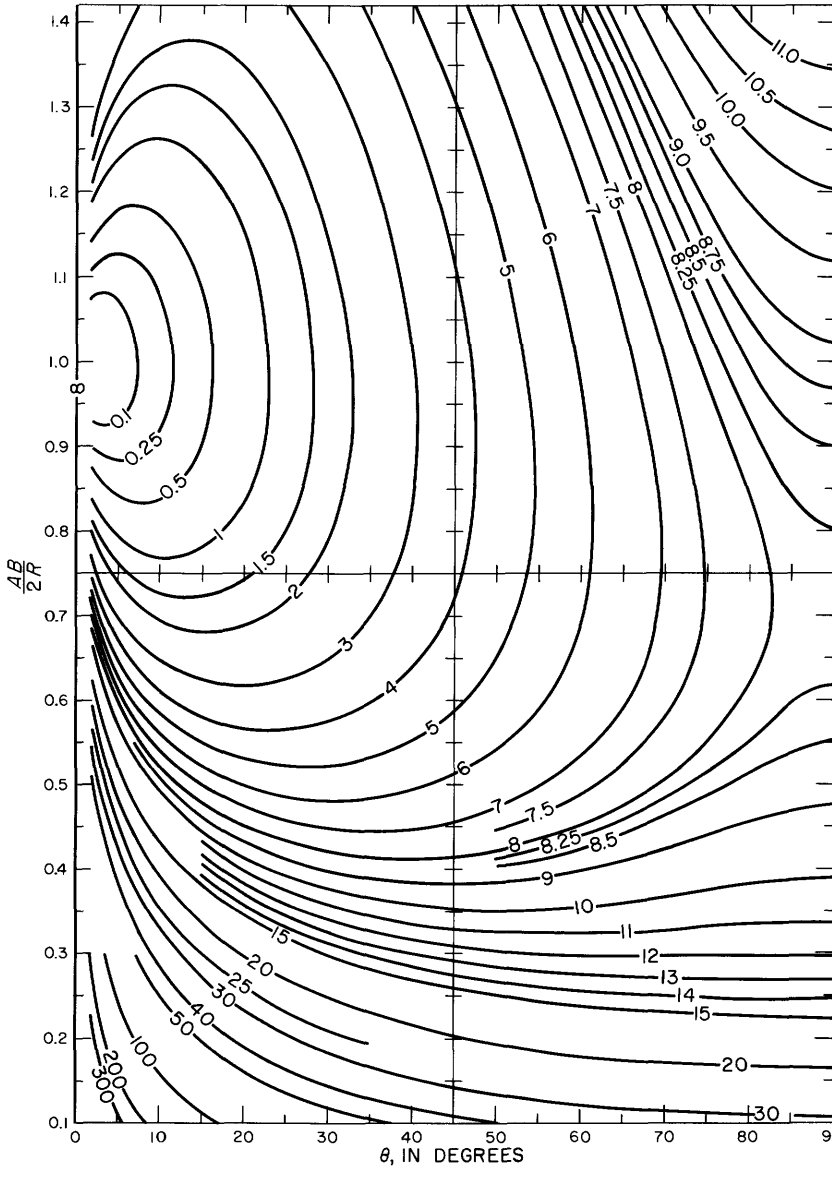

FIGURE 3.—Nomogram for evaluating the factor A_θ of the azimuthal array. Values for A_θ given on curves. AB, distance between current electrodes; R, distance between centers of bipole and dipole; θ, angle between current electrode, center of bipole, and center of dipole; MN, distance between measuring electrodes. ($K_\theta = K^* A_\theta$; $K^* = R^2/MN$.)

Therefore the present nomogram for A_θ is different from that of Berdichevskii not only in the range of $AB/2R$ and θ, but also by a factor for $4R/AB$ in the value of A_ϑ; this further simplifies the evaluation of K^*_θ (compare eq 10 and 12) and therefore of K_θ.

SPECIAL AZIMUTHAL ARRANGEMENTS

Two special azimuthal arrangements—the equatorial and the L-shaped—are of practical interest.

THE EQUATORIAL ARRANGEMENT

The equatorial arrangement has been used rather extensively in the Soviet Union and has proved to be an effective tool in deep resistivity exploration (Berdichevskii and Zagarmistr, 1958; Yakoubovskii and Lyakhov, 1964; Zohdy, 1966; Zohdy and Jackson, 1966). In this special arrangement the angle θ is always equal to 90°. Furthermore, the perpendicularity of MN to R ($\phi=\pi/2$), a condition of the azimuthal arrangement, is also maintained. During the sounding process, the dipole MN is moved away from the bipole AB along the perpendicular bisector of AB. This perpendicular bisector may be regarded as an equator to the poles at A and B; hence the name "equatorial arrangement."

Under these conditions equation 7 reduces to

$$\rho_{\theta=90^\circ}=\rho_{eq}=\frac{R^2}{MN}\frac{\pi}{\left(\frac{AB}{2R}\right)}\left[1+\left(\frac{AB}{2R}\right)^2\right]^{3/2}\frac{\Delta V^{A,B}_{MN}}{I}. \tag{14}$$

According to equation 14, the geometric factor K_{eq} may be expressed as follows

$$K_{eq}=K^*_{eq}A_{eq},$$

where

$$K^*_{eq}=\frac{R^2}{MN}$$

and

$$A_{eq}=\frac{\pi}{\left(\frac{AB}{2R}\right)}\left[1+\left(\frac{AB}{2R}\right)^2\right]^{3/2}. \tag{15}$$

The value of A_{eq} for $0.1\leq(AB/2R)\leq 10$ can be determined easily from the curve in figure 4. The curve $A_{eq}=f(AB/2R)$ exhibits a minimum at $AB/2R=0.7071$, which is easily determined by differentiating equation 15, setting the result equal to zero, and solving for $AB/2R$. The existence of a minimum value for A_{eq} does not, however, mean that the geometric factor $K_{eq}=(R^2/MN)A_{eq}$ attains a minimum value at $AB/2R\simeq 0.71$. In fact, the factor K_{eq} increases continuously, as expected, as R increases.

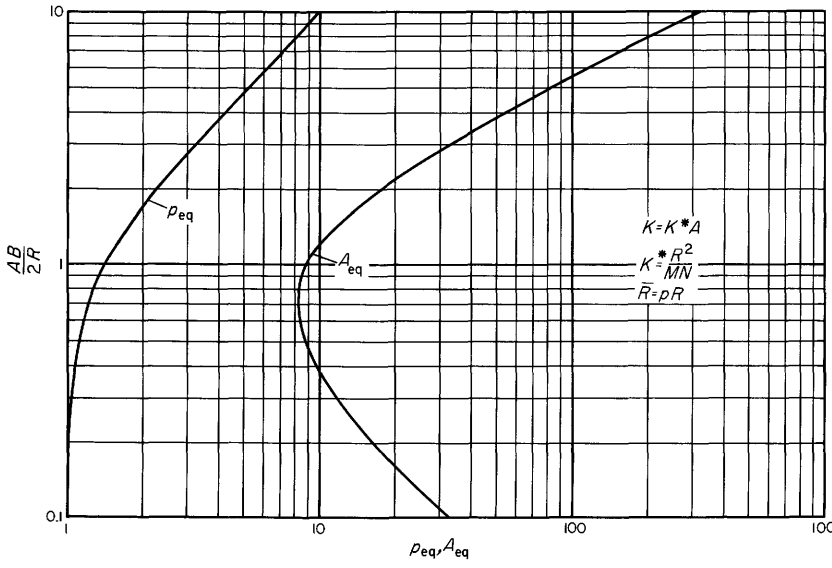

FIGURE 4.—Nomogram for evaluating the factor A_{eq} of the equatorial array ($K^*=R^2/MN$). AB, distance between current electrodes; R, distance between centers of bipole and dipole; $\overline{R}$, distance between current electrode and center of dipole (effective spacing); MN, distance between measuring electrodes; K, geometric factor; p, effective spacing factor $\left(p=\sqrt{1+\left(\frac{AB}{2R}\right)^2}\right)$.

Equation 14 is a special case of equation 7 which in turn is valid only provided $MN \leq 0.1AO$ (see eq 2). However, the general expression for the resistivity, using the equatorial arrangement, may simply be given by

$$\rho_{eq}=\pi \frac{AM\,AN}{AN-AM}\frac{\Delta V_{MN}^{A,B}}{I} \tag{16}$$

or

$$K_{eq}=\pi \frac{AM\,AN}{AN-AM}. \tag{17}$$

For the purpose of computation, equation 17 may be written as

$$K_{eq}=\pi R \frac{\sqrt{\left[1+\left(\frac{AB}{2R}-\frac{MN}{2R}\right)^2\right]\left[1+\left(\frac{AB}{2R}+\frac{MN}{2R}\right)^2\right]}}{\sqrt{1+\left(\frac{AB}{2R}+\frac{MN}{2R}\right)^2}-\sqrt{1+\left(\frac{AB}{2R}-\frac{MN}{2R}\right)^2}}. \tag{18}$$

where in equation 17

$$AM=\sqrt{R^2+\left(\frac{AB}{2}-\frac{MN}{2}\right)^2}$$

and

$$AN=\sqrt{R^2+\left(\frac{AB}{2}+\frac{MN}{2}\right)^2}.$$

Equation 18, in contrast to equation 14, does not imply any restrictions on the length of MN with respect to AO and BO. However, if a component of the electric field is to be approximately measured, then for $AB/2R \leq 1$, $MN/2R \leq 0.1$; and for $1 \leq (AB/2R) \leq 10$, $0.1 \leq (MN/2R) \leq 4$.

In order to simplify computations, equation 18 can also be expressed as the product of two factors,

$$K_{eq} = K^{**}_{eq} A^{*}_{eq},$$

where

$$K^{**}_{eq} = R \tag{19}$$

and

$$A^{*}_{eq} = \pi \frac{\sqrt{\left[1+\left(\frac{AB}{2R}-\frac{MN}{2R}\right)^2\right]\left[1+\left(\frac{AB}{2R}+\frac{MN}{2R}\right)^2\right]}}{\sqrt{1+\left(\frac{AB}{2R}+\frac{MN}{2R}\right)^2}-\sqrt{1+\left(\frac{AB}{2R}\right)-\frac{MN}{2R}\Big)^2}}. \tag{20}$$

The variation of the factor A^{*}_{eq} as a function of $0.1 \leq (AB/2R) \leq 1.5$ for $0.01 \leq (MN/2R) \leq 0.1$ is shown in the nomogram in figure 5.

Interpolation between the various curves for $MN/2R$ can be made by using a logarithmic scale (rotated through 180°) of the same modulus as the one on which the curves are plotted. For example, let $R = 1{,}000$

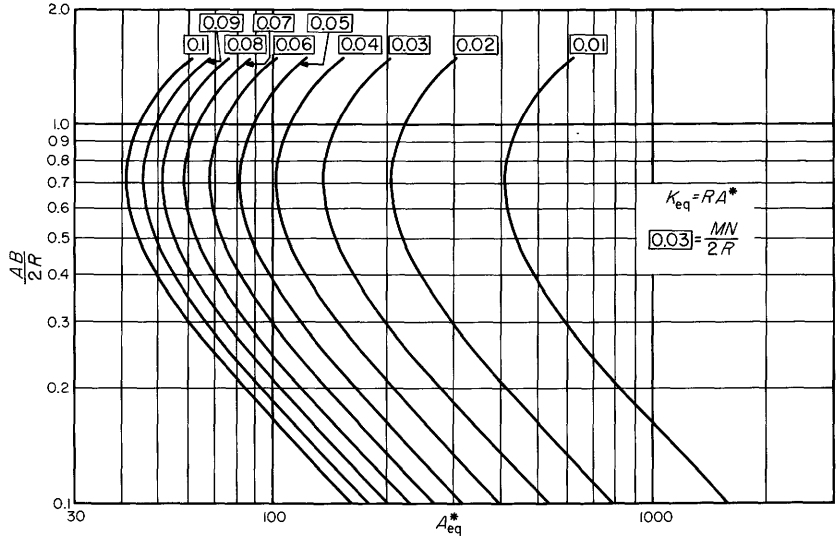

FIGURE 5.—Nomogram for evaluating the factors A^{*}_{eq} of the equatorial array ($K^{**}=R$). AB, distance between current electrodes; R, distance between centers of bipole and dipole; K, geometric factor; MN, distance between measuring electrodes.

meters, $AB=1{,}000$ meters, and $MN=34$ meters; then $AB/2R=0.5$, $MN/2R=0.017$, $A^*\simeq 257$, and $K_{eq}=RA^*=2.57\times 10^5$ meters. Berdichevskii (1954) and Berdichevskii and Petrovskii (1956) presented another nomogram to assist in the computation of K_{eq}. Their corresponding expression for K^{**} is given by

$$K^{**}=C=\frac{R^3}{AB\ MN}10^3,$$

which is not as simple as the one given in equation 19.

EFFECTIVE SPACING OF THE EQUATORIAL ARRANGEMENT

If an equatorial array is placed at the surface of a horizontally stratified laterally homogeneous and isotropic half space, then because of the symmetry of the arrangement

$$\frac{\Delta V^{A,B}_{M,N}}{I}=2\frac{\Delta V^{A}_{MN}}{I}.$$

Therefore, in accordance with equation 16

$$\rho_{eq}=2\pi\frac{AM\ AN}{AN-AM}\frac{\Delta V^{A}_{MN}}{I}=\rho_{AMN}. \tag{21}$$

In other words, by using the equatorial arrangement at a spacing $\overline{R}=AO=R\sqrt{1+\left(\frac{AB}{2R}\right)^2}$, one measures the same magnitude of apparent resistivity as by using a three-electrode AMN (half-Schlumberger) array at a spacing AO. The distance $AO=\overline{R}$ of the equatorial array is referred to as the effective spacing because, by plotting the apparent resistivity as a function of $AO=\overline{R}$, one can use the available albums of theoretical Schlumberger sounding curves for horizontally stratified media to interpret equatorial sounding curves. The Schlumberger theoretical curves cannot be used, however, to interpret the results of any other array (including dipole-dipole ones, except for the azimuthal dipole-dipole) even when the resistivity is plotted as a function of the effective spacing as defined by Al'pin (1950) or by Keller (1966). The effective spacings of other arrays only translate the sounding curve such that the inverse slope of the terminal right-hand rising branch (indicating the detection of a highly resistive basement) would be equal to the total longitudinal conductance of the section above the basement.

In the equatorial arrangement, the effective spacing, $\overline{R}$, is related to the spacing R by

$$\overline{R}=pR,$$

where

$$p=\sqrt{1+\left(\frac{AB}{2R}\right)^2}. \tag{22}$$

Variation of the effective spacing factor, p, as function of $(AB/2R)$ is given in figure 4 together with the variation of the factor A_{eq}.

At the present time, it is customary in the United States and Canada to use the foot as a unit of distance and depth and the ohm-meter as a unit of resistivity. To facilitate the fieldwork with the equatorial arrangement, in tables 1, 2, and 3 the parameters R, $AB/2$, $MN/2$, and $\overline{R}$ are in feet, and K_{eq} is in meters (the current I is to be measured in milliamps and ΔV in millivolts). In this way when the current I is made numerically equal to the appropriate value of K_{eq}, the ΔV, measured in millivolts, will be numerically equal to the resistivity, in ohm-meters.

TABLE 1.—*Geometric factor of the equatorial array for variable* AB/2

[R, $AB/2$, $MN/2$, and $\overline{R}$, in feet; K_{eq}, in meters. Modified from Berdichevskii and Petrovskii, 1956]

R	$AB/2$	$MN/2$	$\overline{R}$	$K_{eq}\times10^3$	$\frac{K}{2}\times10^3$	$\frac{K}{3}\times10^3$	$\frac{K}{4}\times10^3$	$\frac{K}{5}\times10^3$	$\frac{K}{7}\times10^3$
200	200	20	283	2.665	1.332	0.8883	0.6662	0.533	0.3807
400	200	25	447	8.518	4.259	2.839	2.129	1.704	1.217
400	500	25	640	10.026	5.013	3.342	2.506	2.005	1.432
600	200	50	632	12.11	6.055	4.036	3.027	2.422	1.730
800	200	50	825	26.8	13.4	8.933	6.700	5.36	3.829
800	500	50	943	16.02	8.01	5.340	4.005	3.204	2.289
1,200	500	50	1,300	41.79	20.89	13.93	10.45	8.358	5.970
1,600	500	150	1,676	30.19	15.10	10.06	7.547	6.038	4.313
2,000	500	200	2,061	42.09	21.04	14.03	10.52	8.418	6.013
2,000	1,500	200	2,500	24.89	12.44	8.296	6.222	4.978	3.556
3,000	500	200	3,041	134.75	67.37	44.92	33.69	26.95	19.25
3,000	1,500	200	3,340	59.95	29.97	19.98	14.99	11.99	8.564
4,500	1,500	300	4,743	112.9	56.45	37.63	28.22	22.58	16.13
6,000	1,500	300	6,184	251.0	125.5	83.66	62.75	50.20	35.86
8,000	1,500	400	8,139	428.8	214.4	142.9	107.2	85.76	61.26
10,000	1,500	400	10,112	821.5	410.75	273.8	205.4	164.3	117.4
12,000	1,500	400	12,091	1,405	702.5	468.3	351.2	281.0	200.7

TABLE 2.—*Geometric factor of the equatorial array for* AB/2=*2,000 feet*

[R, $MN/2$, and $\overline{R}$, in feet; K_{eq}, in meters]

R	$MN/2$	$\overline{R}$	$K_{eq}\times10^3$
2, 000	200	2, 830	26. 65
4, 000	250	4, 470	85. 18
6, 000	500	6, 320	121. 1
8, 000	500	8, 250	269. 809
10, 000	500	10, 198	509. 507
12, 000	600	12, 165	720. 873
13, 000	600	13, 153	910. 593
14, 000	600	14, 142	1, 131. 441
16, 000	800	16, 124	1, 259. 031
20, 000	1, 000	20, 099	1, 951. 020

TABLE 3.—*Geometric factor of the equatorial array for* AB/2= *4,000 feet*

[R, in feet; value in parentheses, in miles. $MN/2$ and $\overline{R}$, in feet. K_{eq}, in meters]

R	$MN/2$	$\overline{R}$	$K_{eq}\times10^3$
2, 640 (0.5)	200	4, 793	65. 85
3, 960 (0. 75)	200	5, 628	106. 75
5, 280 (1)	300	6, 624	116. 11
6, 600 (1. 25)	400	7, 717	137. 85
7, 920 (1. 5)	400	8, 873	209. 44
10, 560 (2)	400	11, 292	431. 52
10, 560 (2)	600	11, 292	288. 21
13, 200 (2.5)	600	13, 793	524. 73
15, 840 (3)	1, 000	16, 337	524. 57
18, 480 (3.5)	1, 000	18, 908	812. 25
21, 120 (4)	1, 500	21, 494	798. 01
21, 120 (4)	2, 000	21, 494	531. 92
26, 400 (5)	2, 000	26, 701	1, 147. 35
31, 680 (6)	2, 000	31, 932	1, 959. 69

L-SHAPED AZIMUTHAL ARRANGEMENT

In this second special azimuthal arrangement, the perpendicularity of MN to R is maintained as usual while the center 0 of the dipole MN is shifted along a line perpendicular to AB, at one of the current electrodes (fig. 6). Thus, the system acquires an L-shaped configuration, where

$$\cos\theta=\frac{AB}{2R}$$

and

$$\sin\theta=\sqrt{1-\left(\frac{AB}{2R}\right)^2}.$$

Hence from equation 8, the geometric factor $K_{\theta L}$ may be written in the form

$$K_{\theta L}=K^*_{\theta L}A_{\theta L},$$

where

$$K^*_\theta=\frac{R^2}{MN} \tag{23}$$

and

$$A_{\theta L}=\frac{2\pi}{\sqrt{1-\left(\frac{AB}{2R}\right)^2}}\frac{1}{\left(\frac{AB}{2R}\right)}\left(\frac{1}{\left[1+3\left(\frac{AB}{2R}\right)^2\right]^{-3/2}+\left[1-\left(\frac{AB}{2R}\right)^2\right]^{-3/2}}\right). \tag{24}$$

The variation of $A_{\theta L}$ as a function of the ratio $\frac{y}{(AB/2)}$ (fig. 6) is shown in figure 7 (together with the curves for A_{xL} and A_{yL}), where y is the distance along the perpendicular to one of the current electrodes.

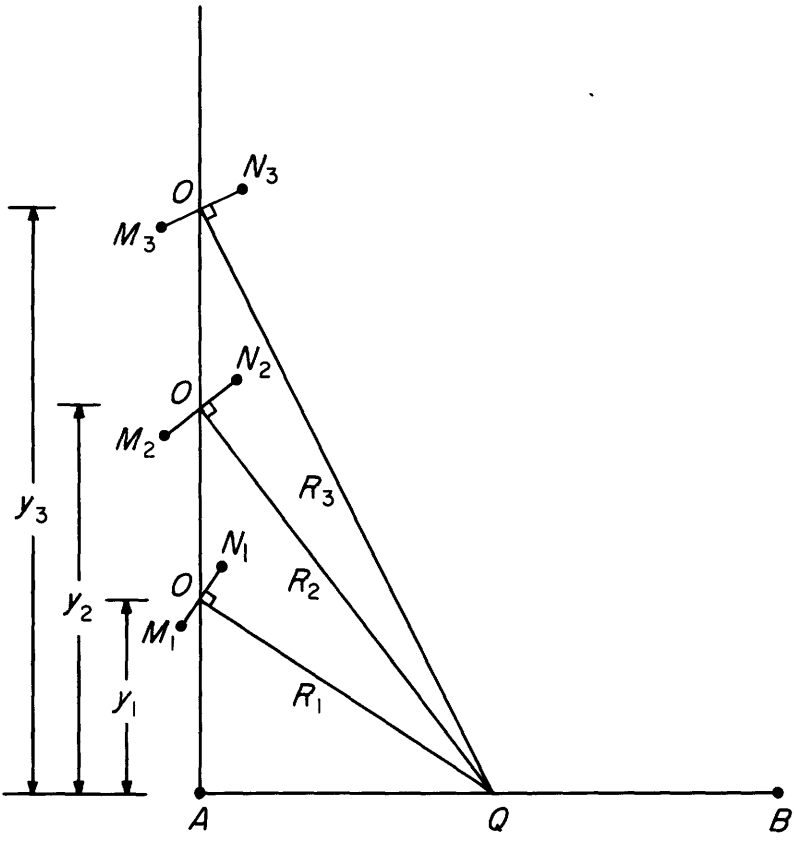

FIGURE 6.—The L-shaped azimuthal array. A and B, current electrodes; Q, center of bipole; M and N, measuring electrodes; O, center of dipole; R, distance between center of bipole and dipole; y, distance along the perpendicular between current electrode and center of dipole.

GEOMETRIC FACTOR OF THE PARALLEL ARRANGEMENT

In the parallel arrangement, the potential dipole MN is always kept parallel to the current bipole AB (fig. 8). At $\theta=90°$ the parallel arrangement reduces to the equatorial, and at $\theta=0°$ it reduces to the asymmetric-Schlumberger arrangement (at $R<AB/2$) or to the polar bipole-dipole configuration (at $R>AB/2$).

Following the same procedures discussed for the azimuthal arrangement, it can be easily shown that the geometric factor of the parallel arrangement is

$$K_x=K_x^*A_x, \tag{25}$$

where

$$K_x^*=\frac{R^2}{MN} \tag{26}$$

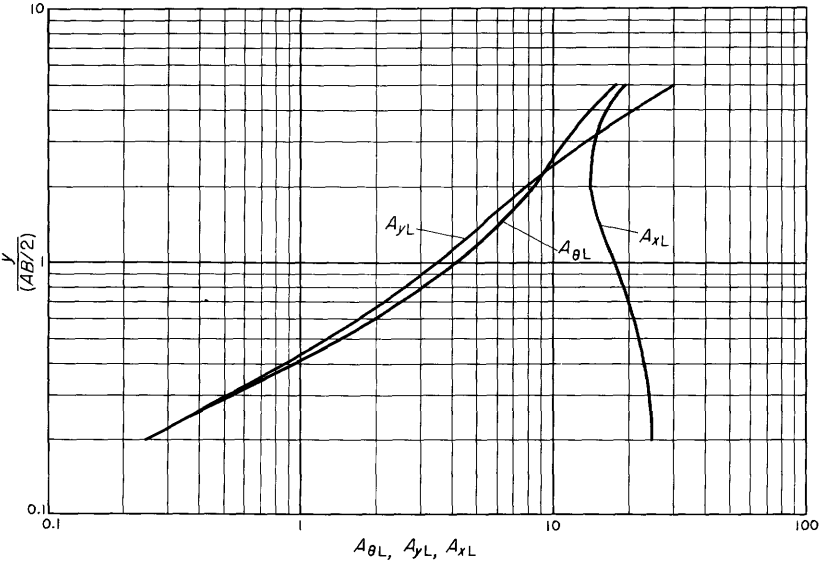

FIGURE 7.—Nomogram for evaluating the factors $A_{\theta L}$, A_{xL}, and A_{yL} of the L-shaped azimuthal, parallel, and perpendicular arrays, respectively. y, distance along the perpendicular between current electrode and center of dipole; AB, distance between current electrodes; R, distance between centers of bipole and dipole; MN, distance between measuring electrodes. ($K_{\theta L}=K^*A_{\theta L}$; $K_{xL}=K^*A_{xL}$; $K_{yL}=K^*A_{yL}$; $K^*=R^2/MN$.)

and

$$A_x=2\pi\left(\left[\frac{AB}{2R}+\cos\theta\right]\left[1+\left(\frac{AB}{2R}\right)^2+2\left(\frac{AB}{2R}\right)\cos\theta\right]^{-3/2}+\left[\frac{AB}{2R}-\cos\theta\right]\left[1+\left(\frac{AB}{2R}\right)^2-2\left(\frac{AB}{2R}\right)\cos\theta\right]^{-3/2}\right)^{-1}. \quad (27)$$

The expression for A_x becomes negative if $\cos\theta > AB/2R$ and the second term is larger than the first. These negative values of A_x result from a reversal in the direction of the electric field component E_x with respect to MN (fig. 8), which leads to the calculation of a negative resistivity.

A nomogram for the evaluation of the factor A_x is shown in figure 9. The value of A_x becomes infinite along a given contour which represents the locus of points ($AB/2R$, θ) where the dipole MN is tangent to an equipotential line. Mathematically, the values of A_x to the right of this contour are positive and those to the left are negative. The values of A_x tend to $+\infty$ when the infinity contour is approached from the right and to $-\infty$ when it is approached from the left.

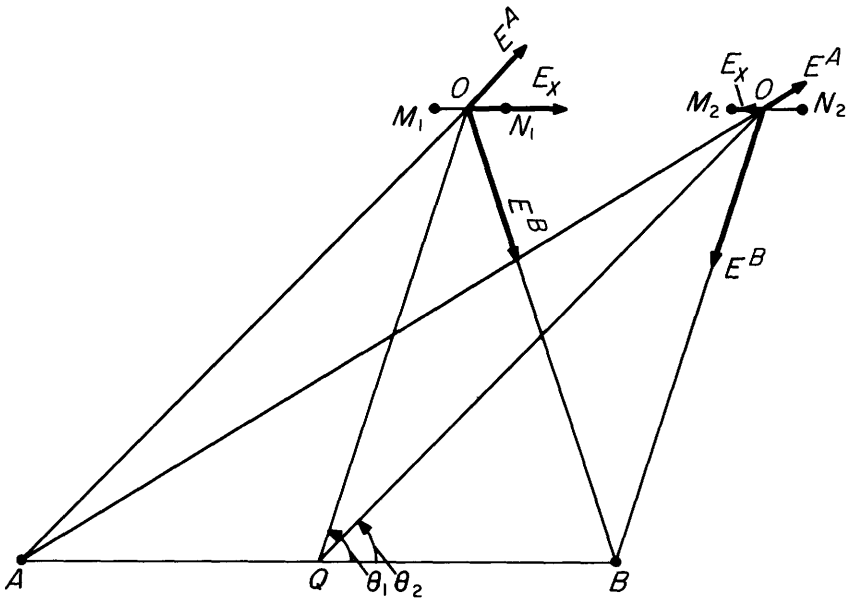

FIGURE 8.—Bipole-dipole parallel array. A and B, current electrodes; Q, center of bipole; M and N, measuring electrodes; O, center of dipole; E, point-source component of the electric field; E_x, parallel component of the electric field.

In contrast to the dipole-dipole parallel array, where the absolute value of the geometric factor becomes infinite only at $\theta=54°44'$ (Al'pin, 1950), in the bipole-dipole array the absolute value of the geometric factor increases indefinitely at different values of the angle θ depending on the value of $AB/2R$. At $AB/2R \leq 0.1$ the bipole-dipole becomes an approximate dipole-dipole, and the geometric factor tends to $\pm\infty$ at $\theta \simeq 54°44'$ (or at arctan $\theta \simeq \sqrt{2}$).

The procedure of evaluating A_x from the given nomogram (fig. 9) is identical with that of the azimuthal arrangement. The part of this nomogram for $AB/2R > 1$ is especially valuable in computing the geometric factor K_x for measurements made with the "rectangle of resistivity" method (Breusse and Astier, 1961).

SPECIAL PARALLEL ARRANGEMENTS

The parallel arrangement coincides with the azimuthal arrangement at $\theta=90°$, and the general expression for A_x (eq 27) reduces to that of the equatorial configuration (eq 15). The L-shaped parallel arrangement may be of interest in exploration, but the polar and asymmetric-Schlumberger configurations are more widely used. In the following, each of these special arrays is briefly discussed.

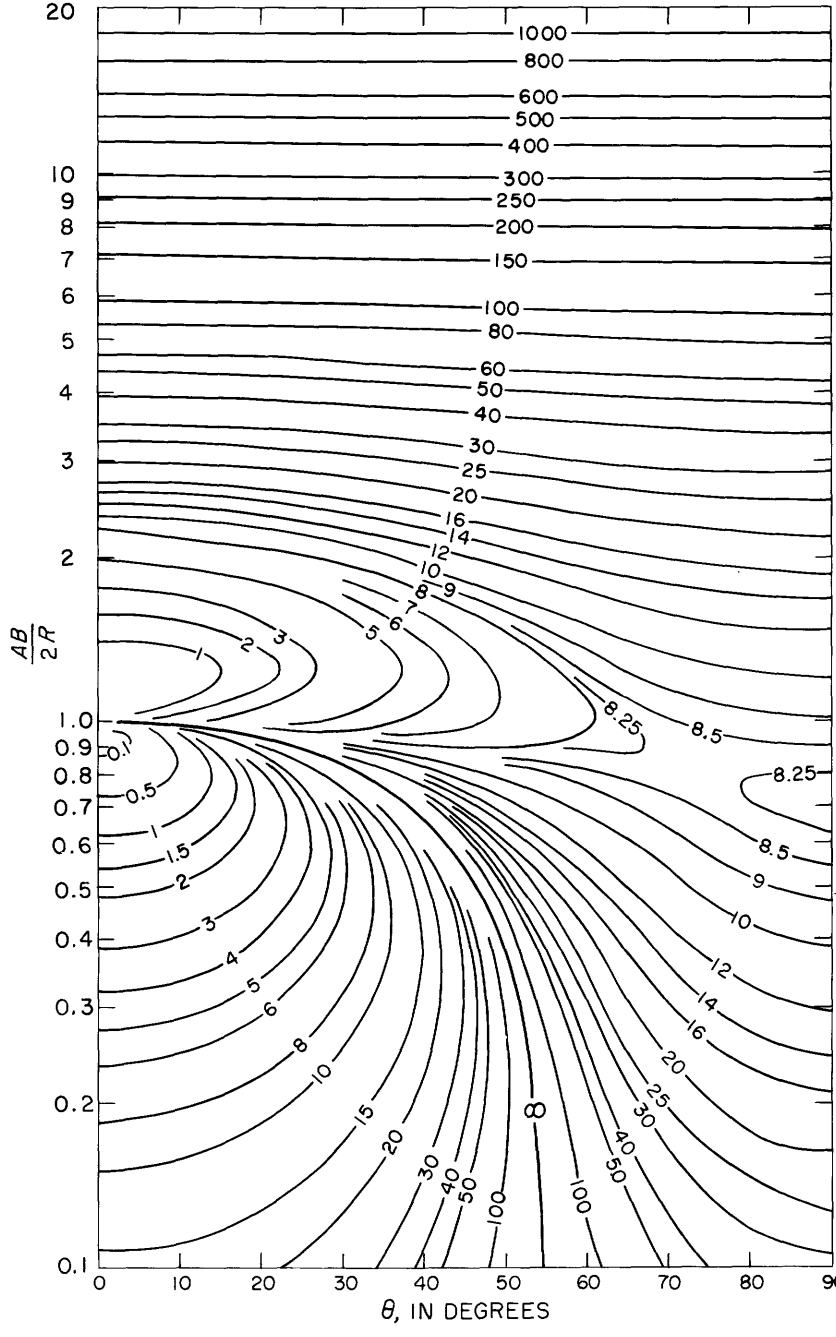

FIGURE 9.—Nomogram for evaluating the factor A_x of the parallel array. Values for A_x given on curves. AB, distance between current electrodes; R, distance between centers of bipole and dipole; θ, angle between current electrode, center of bipole, and center of dipole; MN, distance between measuring electrodes. ($K_x = K^* A_x$; $K^* = R^2/MN$.)

L-SHAPED PARALLEL ARRANGEMENT

In this array, the parallelism of MN to AB is maintained as the point of measurement, O, is moved along a line perpendicular to AB at one of the current electrodes (fig. 10). Therefore, cos $\theta=AB/2R$ and the source at A does not contribute to the electric field component along the direction of MN. Using equations 25, 26, and 27, the geometric factor K_{xL} can be written as

$$K_{xL}=K^*_{xL}A_{xL}, \tag{28}$$

where

$$K^*_x=\frac{R^2}{MN} \tag{29}$$

and

$$A_{xL}=\pi\frac{2R}{AB}\left[1+3\left(\frac{AB}{2R}\right)^2\right]^{3/2}$$
$$=\pi\left(\frac{2y}{AB}\right)\left[1+\left(\frac{AB}{2y}\right)^2\right]^{1/2}\left[1+3\frac{\left(\frac{AB}{2R}\right)^2}{1+\left(\frac{AB}{2y}\right)^2}\right]^{3/2}, \tag{30}$$

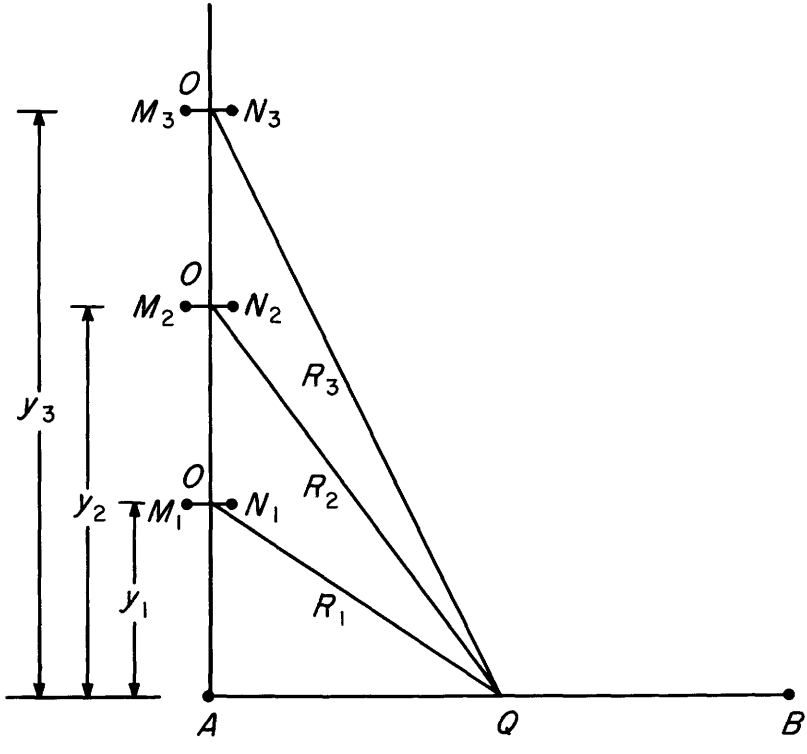

FIGURE 10.—The L-shaped parallel array. A and B, current electrodes; Q, center bipole; M and N, measuring electrodes; O, center of dipole; R, distance between centers of bipole and dipole; y, distance along the perpendicular between current electrode and center of dipole.

where y is the perpendicular distance AO (fig. 10). The factor A_{x_L} may be easily evaluated by using the curve of $A_{x_L}=f\left(\frac{y}{AB/2}\right)$ shown in figure 7.

POLAR AND ASYMMETRIC-SCHLUMBERGER ARRANGEMENTS

In these arrangements, the angle θ is always equal to zero, and hence the measuring dipole is always in line with the current bipole (fig 11). Consequently, $\cos\theta=1$, and the expression for the geometric factor K_x (eq 25) is reduced to

$$K_{asym,p}=K^*A_{asym,p},$$

where

$$K^*=\frac{R^2}{MN}$$

and

$$A_{asym,p}=2\pi\left(\left[1+\frac{AB}{2R}\right]\left[1+\left(\frac{AB}{2R}\right)^2+2\left(\frac{AB}{2R}\right)\right]^{-3/2}+\left[\frac{AB}{2R}-1\right]\left[1+\left(\frac{AB}{2R}\right)^2-2\left(\frac{AB}{2R}\right)\right]^{-3/2}\right)^{-1} \quad (31)$$

or

$$A_{asym,p}=2\pi\frac{\left(\frac{AB}{2R}-1\right)^2}{\pm\left(\frac{AB}{2R}-1\right)^2\pm\left(1+\frac{AB}{2R}\right)^2}. \quad (32)$$

The equation has four roots given by

$$A_{asym(\pm,\pm)}=\pm\frac{\pi\left[\left(\frac{AB}{2R}\right)^2-1\right]^2}{\left(\frac{AB}{2R}\right)^2+1} \quad (33)$$

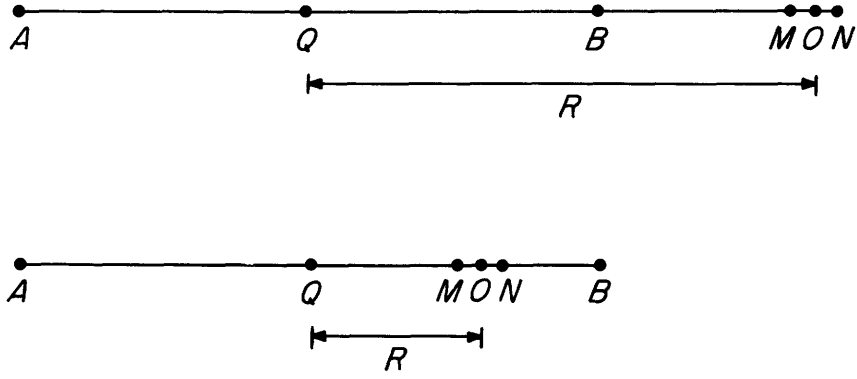

FIGURE 11.—Polar (*upper*) and asymmetric-Schlumberger (*lower*) arrays. A and B, current electrodes; Q, center of bipole; M and N, measuring electrodes; O, center of dipole; R, distance between centers of bipole and dipole.

for $(AB/2R) \geq 1$, and

$$A_{p(\pm,\mp)} = \mp \frac{\pi\left[\left(\frac{AB}{2R}\right)^2 - 1\right]^2}{2\left(\frac{AB}{2R}\right)} \tag{34}$$

for $(AB/2R) \leq 1$.

Equation 33 is used for computing the factor A_{asym} of the asymmetric Schlumberger arrangement $(AB/2R > 1)$. The positive root is for the AMNB arrangement, and the negative root is for the *ANMB* arrangement. Similarly equation 34 is used for computing the factor A_p for the polar arrangement $(AB/2R < 1)$, using the negative root for *ABMN* and the positive root for *ABNM*. In practice, the absolute values of equations 33 and 34 can be used (fig. 12) to avoid the calculation of a negative resistivity, but the distinction between the role of each equation must be emphasized for calculating the correct geometric factors.

The expressions for A_p and A_{asym} both vanish at $AB/2R = 1$, and it is of interest to determine the geometric factors K_p and K_{asym} at $AB/2R =$

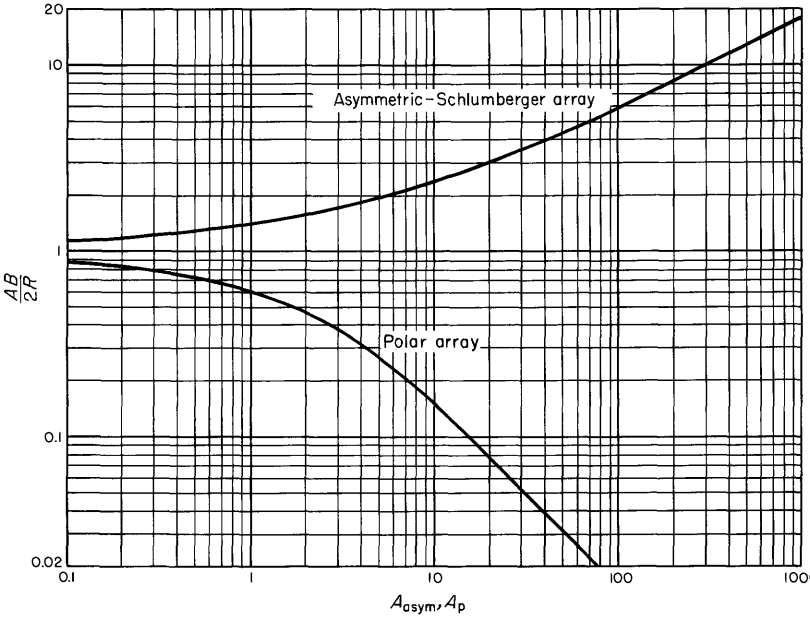

Figure 12.—Nomogram for evaluating the factors A_{asym} and A_p of the asymmetric-Schlumberger and polar arrays, respectively $(K^* = R^2/MN)$. *AB*, distance between current electrodes; *R*, distance between centers of bipole and dipole; *MN*, distance between measuring electrodes.

1. Using the condition $BO \geq 10MN$, where B is the nearest current electrode to the center O of MN, it can easily be shown that for the polar arrangement

$$BO = R - \frac{AB}{2} = R\left[1 - \frac{AB}{2R}\right] \geq 10MN,$$

or

$$MN \leq 0.1R\left[1 - \frac{AB}{2R}\right].$$

Therefore, if, for example, $BO = 100MN$, then

$$K_p = 100 \frac{R}{\left(1 - \frac{AB}{2R}\right)} \frac{\left[\left(\frac{AB}{2R}\right) - 1\right]^2}{2\left(\frac{AB}{2R}\right)}.$$

At $AB/2R = 1$, $K_p = \frac{0}{0}$. Therefore, using L'Hopital's rule

$$\lim_{\frac{AB}{2R} \to 1} K_p = \lim_{\frac{AB}{2R} \to 1} \frac{\frac{d}{d\left(\frac{AB}{2R}\right)}\left(100\pi R\left[\left(\frac{AB}{2R}\right)^2 - 1\right]^2\right)}{\frac{d}{d\left(\frac{AB}{2R}\right)}\left(2\left(\frac{AB}{2R}\right)\left(1 - \frac{AB}{2R}\right)\right)} = 0.$$

Similarly, by using the same type of analysis it can also be shown that $K_{asym} = 0$ at $AB/2R = 1$. Therefore both K_p and K_{asym} become identically zero at $AB/2R = 1$. The general geometric factor K_x of the parallel arrangement may, however, become infinite if the angle $\theta \neq 0$ and $AB/2R \to 1$. (See fig. 9.)

GEOMETRIC FACTOR OF THE PERPENDICULAR ARRANGEMENT

In the perpendicular arrangement the direction of MN is always maintained at right angles to AB (fig. 13). The analysis for evaluating the geometric factor K_y is similar to that of the azimuthal configuration. Hence it can be shown that

$$K_y = K_y^* A, \tag{35}$$

where

$$K_y^* = \frac{R^2}{MN} \tag{36}$$

and

$$A_y = \frac{2\pi}{\sin\theta}\left(\left[1 + \left(\frac{AB}{2R}\right)^2 - 2\left(\frac{AB}{2R}\right)\cos\theta\right]^{-3/2} - \left[1 + \left(\frac{AB}{2R}\right)^2 + 2\left(\frac{AB}{2R}\right)\cos\theta\right]^{-3/2}\right)^{-1}. \tag{37}$$

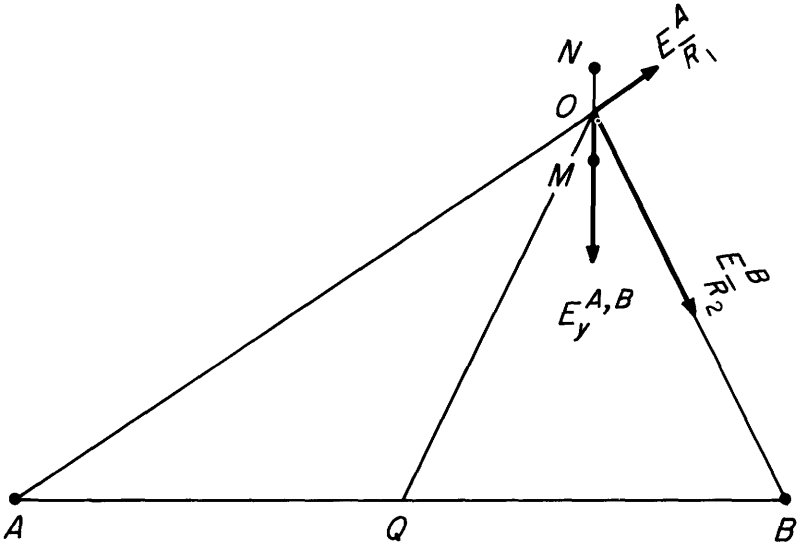

FIGURE 13.—Bipole-dipole perpendicular array. A and B, current electrodes; Q, center of bipole; M and N, measuring electrodes; O, center of dipole; E, point-source component of the electric field; E_y, perpendicular component of the bipole electric field.

The nomogram for the evaluation of the factor A_y is given in figure 14. From equation 37, A_y becomes infinite at $\theta=0$ and $\pi/2$, which indicates that at these angles, MN is alined along an equipotential line. The perpendicular arrangement is most useful in the L-shaped configuration.

L-SHAPED PERPENDICULAR ARRANGEMENT

The perpendicularity of MN with respect to AB is maintained, and the measurements are carried out along a line perpendicular to one of the current electrodes (fig. 15). Therefore

$$\cos\theta=\frac{AB}{2R} \tag{38}$$

and

$$\sin\theta=\sqrt{1-\left(\frac{AB}{2R}\right)^2}. \tag{39}$$

Therefore, using equation 37, the geometric factor K_y can be written as

$$K_{y\mathrm{L}}=K^*_{y\mathrm{L}}A_{y\mathrm{L}}, \tag{40}$$

where

$$K^*_{y\mathrm{L}}=\frac{R^2}{MN} \tag{41}$$

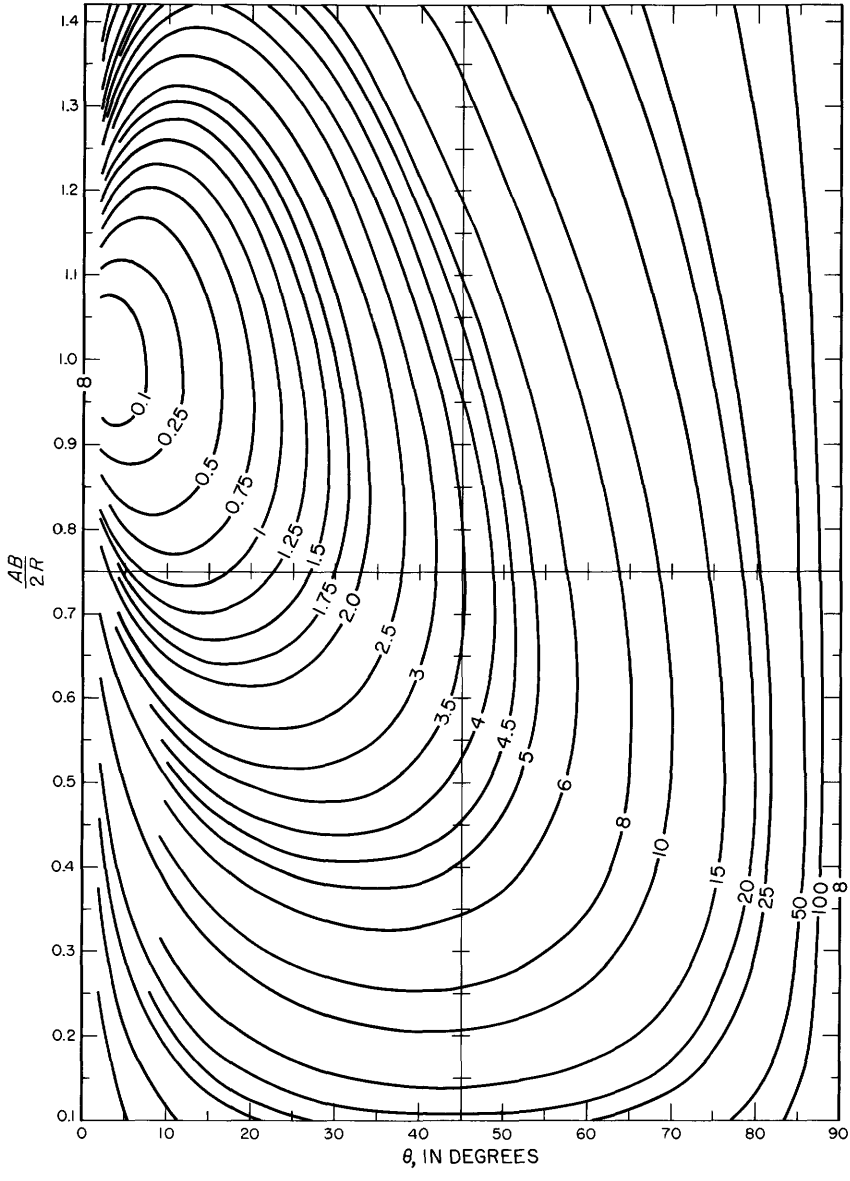

FIGURE 14.—Nomogram for evaluating the factor A_y of the perpendicular array. Values for A_y given on curves. AB, distance between current electrodes; R, distance between centers of bipole and dipole; θ, angle between current electrode, center of bipole, and center of dipole. ($K_y = K^* A_y$; $K^* = R^2/MN$).

and

$$A_{yL} = \frac{2\pi}{\sqrt{1-\left(\frac{AB}{2R}\right)^2}} \left(\left[1-\left(\frac{AB}{2R}\right)^2 \right]^{-3/2} - \left[1+3\left(\frac{AB}{2R}\right)^2 \right]^{-3/2} \right)^{-1}. \qquad (42)$$

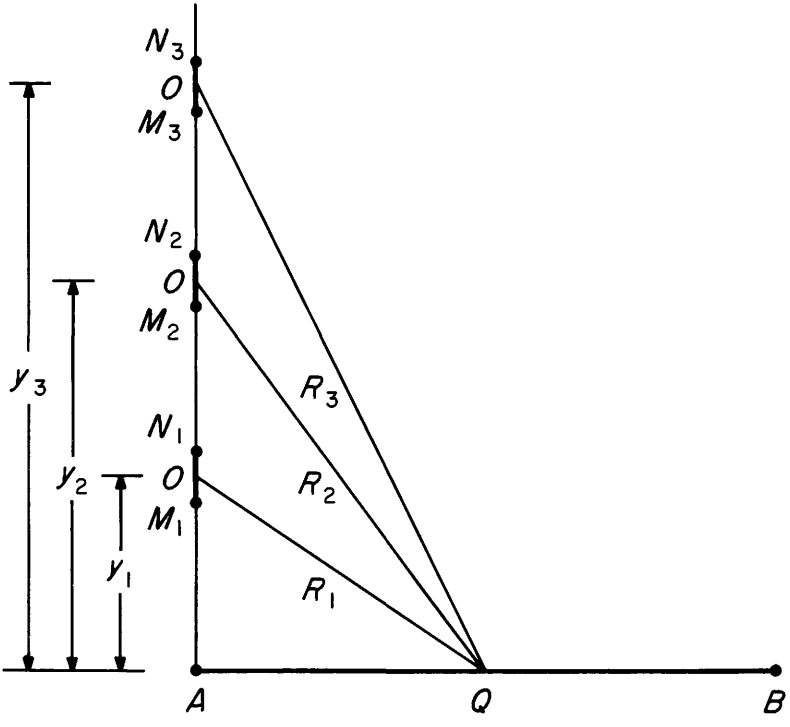

FIGURE 15.—The L-shaped perpendicular array. A and B, current electrodes; Q, center of bipole; M and N, measuring electrodes; O, center of dipole; R, distance between centers of bipole and dipole; y, distance along perpendicular between current electrode and center of dipole.

Substituting $\dfrac{\left(\dfrac{AB}{2y}\right)^2}{1+\left(\dfrac{AB}{2y}\right)^2}$ (fig. 15) for $\left(\dfrac{AB}{2R}\right)^2$

in equation 42, the value of A_{yL} may be plotted as a function of $\left(\dfrac{y}{AB/2}\right)$ as shown in figure 7.

CONCLUSIONS

Formulas for the geometric factors of bipole-dipole arrays are fairly complex, making routine computations very tedious. Most of the computations must be carried out to five significant figures for the final results to be of practical value. Consequently the computations should be made by an electronic computer. The results of such computations, presented here in the form of nomograms, reduce the necessary calculations considerably. The values of the various geometric factors, determined with the aid of the given nomograms, are generally

sufficiently accurate for evaluating field resistivity data, using any of the considered electrode configurations.

REFERENCES CITED

Alekseev, A. M., Berdichevskii, M. N., and Zagarmistr, A. M., 1957, [The use of new methods of electrical exploration in Siberia]: Prikladnaya Geofizika, no. 18, p. 103–127 (in Russian); English translation *in* Applied Geophysics, U.S.S.R., 1962, Pergamon Press, p. 196–222.

Al'pin, L. M., 1950, [The theory of dipole sounding]: Moscow, Gostoptekhizdat, 88 p. (in Russian); English translation *in* Keller, G. V., 1966, Dipole methods for measuring earth conductivity, New York, Consultants Bur., p. 1–60.

Anderson, L. A., and Keller, G. V., 1966, Experimental deep resistivity probes in the central and eastern United States: Geophysics, v. 31, p. 1105–1122.

Berdichevskii, M. N., 1954, [Nomograms for determining the geometric factor for an equatorial array]: Razved. i Promyslovaya Geofizika, v. 10 (in Russian).

——— 1957, [The method of curved electrical probes]: Prikladnaya Geofizika, no. 18, p. 128–144 (in Russian); English translation *in* Applied Geophysics, U.S.S.R., 1962, Pergamon Press, p. 223–240.

Berdichevskii, M. N., and Petrovskii, A. D., 1956, [Procedures of bilateral equatorial soundings]: Prikladnaya Geofizika, no. 14, p. 97–114 (in Russian).

Berdichevskii, M. N., and Zagarmistr, A. M., 1958, [Methods of interpreting dipole resistivity soundings]: Prikladnaya Geofizika, no. 19, p. 57–108 (in Russian); English translation *in* Keller, G. V., 1966, Dipole methods for measuring earth conductivity, New York, Consultants Bur., p. 79–113.

Bordovskii, V. P., 1958, [The determination of the coefficients of dipole arrangements in the case of curvilinear soundings]: Razved. i Promyslovaya Geofizika, v. 24, p. 24–27 (in Russian).

Breusse, J. J., and Astier, J. L., 1961, Etude des diapirs en Alsace et Baden-Wurtemberg par la methode du rectangle de resistivite: Geophys. Prosp., v. 9, p. 444–458.

Cantwell, T., Nelson, P., Webb, J., and Orange, A. S., 1965, Deep resistivity measurements in the Pacific Northwest: Jour. Geophys. Research, v. 70, p. 1931–1937.

Cantwell, T., and Orange, A. S., 1965, Further deep resistivity measurements in the Pacific Northwest: Jour. Geophys. Research, v. 70, p. 4068–4072.

Deppermann, K., 1954, Die Abhangigkeit des scheinbaren Widerstandes vom Sondenabstand bei der Vierpunkt-Methode: Geophys. Prosp., v. 2, p. 262–273.

Heiland, C. A., 1940, Geophysical exploration: New York, Prentice-Hall, 1013 p.

Jackson, D. B., 1966, Deep resistivity probes in the southwestern United States: Geophysics, v. 31, p. 1123–1144.

Keller, G. V., 1966, Dipole method for deep resistivity studies: Geophysics, v. 31, p. 1088–1104.

Yakoubovskii, U. V., and Lyakhov, L. L., 1964, Elektrorazvedka [Electrical prospecting]: Moscow, Izdatel'stvo "NEDRA" (publisher) [Mineral resources], 414 p.

Zohdy, A. A. R., 1964, Earth resistivity and seismic refraction investigations in Santa Clara County, California: Stanford Univ. Ph. D. dissert. 132 p.

——— 1966, Geoelectrical exploration for ground water in the southwestern United States [abs.]: Geophysics, v. 31, p. 1216.

Zohdy, A. A. R., and Jackson, D. B., 1966, Application of resistivity soundings for ground-water investigations in Hawaii [abs.]: Geophysics, v. 31, p. 1216.

U.S. GOVERNMENT PRINTING OFFICE: 1970 O—380-460